Date of publication xxxx 00, 0000, date of current version xxxx 00, 0000.

Digital Object Identifier 10.1109/ACCESS.000.DOI

Enhanced interference management for 6G in-X subnetworks

RAMONI ADEOGUN[1], (Senior Member, IEEE), GILBERTO BERARDINELLI[1], (Senior Member, IEEE), AND PREBEN MOGENSEN[1,2] (Member, IEEE)

[1]Department of Electronic Systems, Aalborg University, Aalborg, Denmark (e-mail: [ra,gb,pm]@es.aau.dk)
[2]Nokia Bell Labs, Aalborg, Denmark (e-mail: preben.mogensen@nokia-bell-labs.com)

Corresponding author: Ramoni Adeogun (e-mail: ra@es.aau.dk).

This work is supported by the Danish Council for Independent Research, grant no. DFF 9041- 00146B.

ABSTRACT Short-range low-power 6th generation (6G) in-X subnetworks are proposed as a viable radio concept for supporting extreme communication requirements in emerging applications such as wireless control of robotic arms and control of critical on-body devices, e.g. wireless heart pacemaker. For these applications, ultra-high reliability (e.g., above 6 nines) with sub-ms latency must be guaranteed at all spatio-temporal instants. To meet these requirements, radio systems that are robust against fading and interference are crucial. In this paper, we present a comprehensive investigation on technology enablers and techniques for interference mitigation in 6G in-X subnetworks. We present several techniques including blind-repetition with pseudo-random frequency hopping and environment-aware mechanisms for interference management via dynamic channel allocation. We further propose two novel enhancements viz: (1) repetition order adaptation involving real-time selection of the number of repetitions based on current channel conditions; and (2) anticipatory packet duplication in which each subnetwork duplicates its transmission on a secondary channel group whenever it detects the presence of a potentially harmful neighbouring subnetwork. We perform extensive simulations in an industrial factory environment with mobile in-X subnetworks using models and parameters defined by the 3rd Generation Partnership Project (3GPP). Results show that in-X subnetworks requires large bandwidth ($\geq$ 1 GHz), up to 2 packet repetitions and environment-aware interference coordination in order to support packet loss rate below 10^{-6} with a latency $< 100\mu$s. The number of repetitions can however be reduced for systems with survival time greater than the cycle time. The proposed enhancements also result in up to $\times 10^4$ packet loss rate reduction for systems with survival time above 2 cycle times.

INDEX TERMS 6G, in-X subnetworks, industrial control, ultra-reliable low latency communication (URLLC), interference mitigation, resource allocation, survival time, packet duplication, link adaptation

I. INTRODUCTION

COMMUNICATION in industrial control networks [1] requires ultra-high reliability, extremely low and deterministic latency (i.e, with low jitter) as well as high scalability for a large number of inter-connected devices [2], [3] including sensors, controllers, and actuators. The current industrial revolution commonly referred to as industry 4.0 [2] envisions inter-connectivity among all devices within a factory from small sensors (or actuators) to large robots. This vision requires availability of communication networks that are reliable, safe, fast and timely within factories [4].

Traditionally, industrial control networks are based on wired technologies such as fieldbus systems (e.g., process fieldbus (PROFIBUS), P-Net and factory instrumentation protocol (FIP)), and Ethernet fieldbus [2]. However, wireless systems are becoming a defacto choice as key enablers of the industry 4.0 visions. The possibility of wirelessly connecting industrial devices is indeed appealing due to its numerous benefits including deployment, configuration and maintenance flexibility, support for mobility, and reduction in costs associated with cables [4], [5]. As with other applications utilizing wireless connectivity, the shared and dynamic nature of the propagation channel poses significant challenges to the support of reliable and timely data exchange required by industrial control applications.

Despite these challenges, there has been a continuous growth in the number of wireless solutions proposed for industrial applications, see e.g., [6]–[10] and the references

Notation	Description	Notation	Description
$\rho_{nm}^{\ell z}$	SINR on link nm, receive antenna, z and ℓth fading block	$P(t)$	Number of repetitions at time t
ρ_{worst}	Worst case SINR	ρ_{th}	SINR threshold for DCGS
G_t	Mutual coupling graph	K	Number of channel groups
$\mathbf{I}(t)$	Mutual inter-subnetwork interference at time t	$\tilde{R}_{apdp}$	Anticipated achieved rate
$\tilde{R}_{target}$	Target rate	β	Binary transmission success indicator
P_{min}	Minimum number of packet repetitions	P_{max}	Maximum number of packet repetitions
N	Number of subnetworks	M	Number of devices per subnetwork
v	Velocity	γ	Pathloss exponent
σ_s	Shadowing standard deviation	d_c	Correlation distance
ζ	Antenna correlation parameter	$\mathbf{V}$	Toeplitz correlation matrix
L	Number of fading blocks	B	Total bandwidth
N_{ofdm}	Number of OFDM symbols	N_{data}	Number of data carriers per symbol
$\mathbf{g}$	iid circular symmetric random vector	h	Correlated small scale fading gain
τ_{surv}	Survival time	Y_{nm}	Desired/interference power on link nm
σ_n^2	Noise power	$\mathcal{I}$	Set of interfering subnetworks
Z	Number of receive antennas	S	Number of snapshots
r_{sub}	Subnetwork radius	T_{snap}	Snapshot duration
d_{min}	Minimum inter-subnetwork distance	$\mathcal{O}$	Big-O notation

TABLE 1: Notations

therein. Majority of the existing solutions, however, target applications with relatively low communication requirements such as process monitoring in the oil and gas, mining, chemical [11] and paper industries. Common example of such wireless technologies include wireless highway addressable remote transducer (HART) [12], ISA 100.11a [13], IEEE 802.15 [14] and Zigbee [15]. Other enhanced technologies including wireless networks for industrial automation - factory automation (WIA-FA), wireless interface for sensors and actuators (WISA) [16] and real time - wireless fidelity (RT-WiFi) [17] have also been developed. In general, the latencies (or equivalently cycle times) offered by these technologies range from 100 ms for wireless HART and $\sim$ 1 ms for RT-WiFi, allowing for support of less time-critical applications (e.g., process and factory automation) but not more critical applications such as power electronic control and motion control, which are still running over wired real-time Ethernet networks.

Currently, the ultra-reliable low latency communication (URLLC) component of the 5th generation (5G) cellular network (referred to here as 5G-URLLC) is witnessing increased penetration into the industrial domain [18], [19]. This is partly due to its design promise of scaling end-to-end latency down to the sub-ms level. 5G-URLLC aims to provide ~ 0.5 ms latency with reliability above 99.9999 by introducing the concept of mini-slots, larger subcarrier spacings with respect to previous Long Term Evolution (LTE) releases, preemptive scheduling methods, and optimized grant-free access procedures.

Despite the design targets above, the 5G network architecture limits the possibility to reduce the end-to-end latency to a level that is acceptable for critical control applications. The development of wireless alternative to wired real-time Ethernet network for the most critical industrial control applications has therefore remained a major factor in the requirement definition and design of wireless systems towards the 6th generation (6G) wireless era.

In the wireless domain, a major consensus among the multitude of recent vision papers on 6G [20]–[25] is the need to support more demanding services with much higher reliability and low latencies than is currently possible with 5G. Recent works on 6G systems have indeed identified several other revolutionary applications such as high-resolution sensing, pervasive mixed reality, and cyber-physical systems [26]–[28], necessitating extreme performance requirements, e.g., super-short latency (down to 100μs), ultra-high reliability and multi-Gbps data rates [29]–[32].

For example, the works in [29], [30] outlined packet loss rate (PLR) (or equivalently outage probability) and latencies below 10^{-6} and 100μs, respectively, for applications such as industrial control at the sensor-actuator level, intra-vehicle control, in-body networks and intra-avionics communications. Compared to the 5G-URLLC performance targets, these extreme requirements represent a factor of 10 scaling of the latency and reliability.

A radio system concept termed in-X[1] subnetworks comprising of short-range low-per cells deployed inside entities such as robots, vehicles, airplane and human-body to ensure that the extreme connectivity requirements are satisfied even in the absence of connection to a large network infrastructure was recently presented in [29]. The computation for the control operations runs locally in the in-X subnetworks, that must host the necessary edge processing capability. In that respect, in-X subnetworks transcend traditional mobile edge computing (MEC) [33] paradigm by moving such computation even closer to the end devices. Clearly, the envisioned applications for in-X subnetworks represent life critical use-cases necessitating the need to guarantee specified communication requirements everywhere and at all times. Such use-cases can also lead to dense scenarios (e.g., in-X subnetworks inside a large number of cars at a road intersection or inside

[1]The term *in-X* is a consequence of the envisioned use-cases including industrial control at the sensor and actuator level, intra-vehicular communication and in-human body networks, for such subnetworks [29]

human bodies in a crowded environment or inside mobile robots operating in an indoor factory environment or in production modules) leading to potentially high interference levels. Such interference levels may limit the possibility for supporting extreme communication requirements, necessitating novel measures beyond traditional reactive approaches. This has resulted in a number of recently published works on radio resource allocation methods for dense wireless networks with independent in-X subnetworks [34], [35]. In [34], distributed heuristic algorithms were evaluated and compared with a centralized graph coloring (CGC) baseline in dense deployments of in-X subnetworks. Although the heuristics show better performance than random allocation, the high abstraction level in the utilized simulation approach limits the interpretability of the results. In [35], a supervised learning method for distributed channel allocation is proposed. Using the CGC method and the abstract simulation procedure developed in [34], datasets comprising of aggregate interference - channel assignment pairs were collected. The data sets were used to perform offline training of a deep neural network. The trained network was then deployed at each subnetwork for distributed channel group selection. While the results show the potential for learning to perform channel allocation in dense deployments of 6G in-X subnetworks, the results also suffers from the effect of the high level of abstraction as in [34].

Relying on the enabling technologies and radio concepts in [29], [32], we present an interference-robust system design for in-X subnetworks aiming at supporting extreme communication requirements in this paper. We consider a combination of medium access components designed to provide inner resilience to inter-cell interference, with environment-aware mechanisms based on local sensing measurements of aggregate interference power. We further present a comprehensive evaluation of the achievable performance of such networks in typical industrial factory environments with a large number of mobile in-X subnetworks.

As stated above, the focus of this paper is on the radio design and mechanisms for mitigating interference in mobile 6G in-X subnetworks operating in typical industrial environments such that the target performance is guaranteed on a spatio-temporal basis. The main contributions of this paper are as follows:

- We present the first comprehensive study on techniques for interference avoidance, coordination and mitigation in 6G in-X subnetworks.
- We evaluate the potentials of in-built robustness mechanisms including blind repetition of robustly coded packets with pseudo-random frequency hopping for mitigating the adverse effects of interference on the performance of in-X subnetworks.
- We present distributed interference-aware dynamic channel selection (DCA) methods as well as two novel enhancement mechanisms viz: anticipatory packet duplication (APDP) and repetition order adaptation for further improving the transmission reliability, and spectral efficiency of the system. The DCA techniques have been presented in part in our earlier works [34], [35].
- We develop a simulation procedure for evaluating the performance of 6G in-X subnetworks in terms of two key metrics for time-critical transmissions viz: packet loss rate and survival time. Defined by the 3rd Generation Partnership Project (3GPP) [36] as the amount of time that an application with periodic packet arrival pattern (e.g, motion control) can continue without an anticipated packet, survival time is seen as a more distinct quality of service (QoS) metric [37] for industrial control applications. Unlike the works in [29], [34], [35] which rely on an abstract mapping of large scale SINR to outage probability, the simulation procedure developed in this paper explicitly capture instantaneous fading effects including small scale fading, shadowing and pathloss. This makes it possible to evaluate typical communication theoretic key performance indicators.

The remainder of this paper are organized as follows. A brief introduction of industrial 6G in-X subnetworks as well as the main technology enablers is presented in section II followed by a description of the proposed interference management and enhancement mechanisms in section III. Section IV describes the considered industrial scenario, channel model, simulation procedure and performance metrics. The performance evaluation results and computational complexity analysis are presented in section V. A comprehensive discussion of the proposed methods and the evaluation results is given in section VI. Finally, conclusions are drawn in section VII.

In Table 1, we present a summary of the mathematical notations used throughout the rest of this paper.

II. INDUSTRIAL 6G IN-X SUBNETWORKS

6G in-X subnetworks were conceived in [29], [31] as independent short range radio cells to provide seamless support for potentially life-critical applications with extremely high reliability and ultra-low latency, e.g., PLR $< 10^{-6}$ with a maximum latency of $100\ \mu$s even in the absence of connectivity from traditional cellular networks. We consider possible industry 4.0 scenarios where mobile robots equipped with in-X subnetworks are transporting materials over a set of manufacturing stations distributed in an indoor factory hall. These subnetworks are expected to support the most critical applications (such as autonomous control of the precision of robots' movement and obstacle avoidance) currently running over wired real-time Ethernet protocols such as Ethernet for control automation technology (EtherCAT).

We consider a network consisting of multiple independent and uncoordinated in-X subnetworks each with a single controller and multiple sensor-actuator pairs. In addition to traditional control functionalities, the controller acts as the access point (AP) for the sensors and actuators in the subnetwork. The sensors continuously collect measurements and transmit same to the AP which then process it and generate appropriate command(s) to the corresponding actuator. We refer to the sensor - to - AP and AP - to - actuator link as

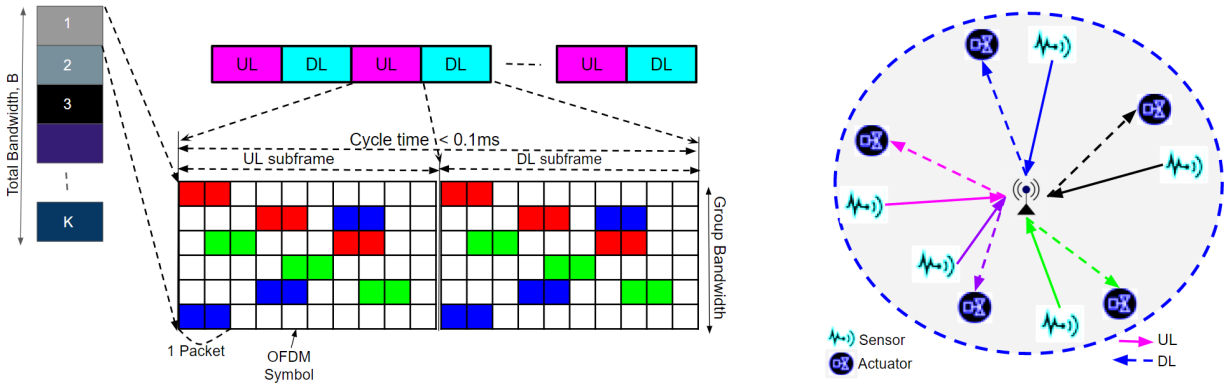

(a) (b)

FIGURE 1: Illustration of the operation of 6G in-X subnetworks for industrial control applications with periodic traffic: (a) bandwidth partitioning and TDD frame structure and (b) a subnetwork with circular coverage area showing the sensor-controller (UL) and controller-actuator (DL) transmissions.

uplink (UL) and downlink (DL), respectively. The ensemble of UL and DL is referred to as a control loop. Considering the latency target for the subnetworks, each control loop has a cycle time, $T_{\text{cycle}} \leq 100\ \mu$s. The cycle time is defined as the total time between the transmission of measurements from a sensor in the UL to the time the corresponding DL control message from the AP to the actuator is processed.

We now present a summary of the main wireless air-interface technologies for achieving the target PLR with latencies below $100\ \mu$s. We refer to [29] for further details.

A. PHYSICAL LAYER (PHY)

In our earlier works [29], [32], we have identified the main physical layer (PHY) features to support the latency requirement in in-X subnetworks. The main features for control applications with deterministic periodic traffic include:

- Orthogonal frequency division multiplexing (OFDM) waveform with large subcarrier spacing (above 240 kHz), and short cyclic prefix (CP) due to the small delay spread associated with short-range transmissions [38].
- Time division duplexing (TDD) due to the its benefits including ease deployment over different spectra, more efficient spectrum utilization, and lower cost relative to frequency division duplexing (FDD), which require paired bands for UL and DL transmissions and duplexers to isolate the paired transmissions [39].
- Multi-antenna transmission to harvest spatial diversity. The spatial diversity gain may however be limited by the small form factors of the devices and AP.

B. MEDIUM ACCESS CONTROL (MAC) AND RADIO RESOURCE MANAGEMENT (RRM)

To guarantee the ultra-high reliability demand, we have identified the following main MAC and RRM features for in-X subnetworks :

- Partitioning of the available bandwidth into multiple channels. The channels are then divided into a number of equal-sized groups.
- Interference coordination via dynamic allocation of resources. At a given time, a subnetwork either select the channel group to operate on based solely on local sensing information or via signalling of channel group assignment from a centralized resource manager.
- Intra-subnetwork interference avoidance via orthogonal transmissions within each subnetwork. The AP manages allocation of orthogonal resources to each device within a channel group.
- Blind packet repetitions combined with hopping within the frequency channels in a channel group. This allows to obtain both interference and frequency diversity.
- Increased interference diversity via pseudo-random patterns for channel hopping. The hopping pattern is randomized at each transmission slot, thereby making the system resilient to adversarial interference from jammers. Such hopping pattern randomization also reduces the persistency of interference from neighbor subnetworks.

C. FRAME STRUCTURE AND NUMEROLOGY

Figure 1a depicts the partitioning of the available bandwidth, B into K equisized channel groups, and an illustration of intra-subnetwork TDD resource structure. At a given time, all transmissions within a subnetwork occur within a single channel group which is allocated using the methods that will be described in section III-A. The AP then instructs each device to repeat its transmission over different channels within the group, according to a specified pseudo-random hopping pattern. The AP also ensures that channels assigned to different devices are orthogonal.

As shown in Figure 1a, the frame is divided in an UL and a DL subframe corresponding to the transmission between sensors and the controller (AP) and between controller and

actuators, respectively. Each transmission can be mapped over a single or more OFDM symbols (e.g. 2 in Figure 1a). To allow sufficient time for channel hopping, a switching gap of a single OFDM symbol is left between successive packet repetitions. This gap also provides the processing time within which transmission decisions are made based on current measurements. Such processing include that of the actual control data and the real-time measurements for repetition adaptation and packet duplication. To meet the latency target, the frame structure is designed with total duration below 100 μs.

Example of possible numerologies considering OFDM transmission with 480kHz subcarrier spacing and a CP of 68 ns is shown in Table 2. The numerologies are based on a symmetric TDD frame structure with 20 OFDM symbols per sub-frame resulting in a cycle time of $\sim$ 84 μs. The numerologies include a processing time of 2.15 μs leading to a total frame duration of $\sim$ 86 μs. In these examples, each packet is mapped over 4 OFDM symbols translating to a total duration of 8.6 μs per transmission. Assuming 4 packet repetitions (including the first hop), the maximum number of supported devices is estimated to be equal to the number of frequency channels per group.

III. INTERFERENCE COORDINATION AND ADAPTATION TECHNIQUES

In this section, we present the investigated interference mitigation and adaptation techniques. We remark here that although all methods described here are applicable to any wireless systems involving dense deployments of mobile subnetworks, the focus of this paper is on industrial 6G in-X subnetworks.

A. ENVIRONMENT AWARE INTERFERENCE COORDINATION

Blind repetition of robustly coded packets and hopping over multiple frequency channels are included in the design of PHY and MAC enablers for 6G in-X subnetworks in order to provide robustness against fading and interference translating to an increase in the communication success. These methods are however, blind to the expected changes in inter-subnetwork interference level due to mobility and variations in the environment. To this end, we investigated methods for dynamically adapting the operational channel group at each subnetwork based on sensing data on the status of all groups in [34]. Specifically, algorithms for dynamic channel group selection (DCGS) were developed. These methods rely on measurements of the worst case SINR, ρ_{worst} measured at either the devices or AP in each subnetwork, and on sensed aggregate interference power averaged over all channels within each group for DCGS decision. Since DCGS decisions are made by the AP, devices need to signal measured SINR levels to the AP which then estimate ρ_{worst} as the minimum SINR over all UL and DL transmissions in a single frame.

TABLE 2: Considered numerology with different number of channels per group

Parameters	Value
Subcarrier spacing (kHz)	480
CP length (ns)	68
CP overhead (%)	3,16
Total OFDM symbol duration (μs)	2,15
OFDM symbols per subframe	20
OFDM symbols per packet transmission	4
Number of frequency channels	6 | 12 | 24 | 36 |
Max. number of packet repetitions	4
Interval between repetitions [OFDM symbols]	1
Max. number of supported loops	6 | 12 | 24 | 36 |
Time for transmitting sensors' data [μs]	40,88
Subframe duration [μs]	43,03
Frame duration [μs]	86,05
Processing time at the controller [μs]	2,15
Cycle time [μs]	83,90

1) Distributed Dynamic Channel Group Selection

In the distributed DCGS (DDCGS) schemes, channel group selection decision is made at each subnetwork whenever ρ_{worst} is less or equal to a specified SINR threshold, ρ_{th}. The SINR threshold can for example be set as that required to guarantee a target rate or equivalently, a target error probability. A summary of the DDCGS methods evaluated in this paper is as follows: If $\rho_{\text{worst}} \leq \rho_{\text{th}}$, do either of the following

- Greedy: select the best channel group, i.e., the group with the lowest detected aggregate interference power;
- Nearest neighbour Conflict Avoidance (NNCA): select a group that is not occupied by $K-1$ nearest neighbours. This method rely on the assumption that each subnetwork is able to obtain information of the channel group occupied by its nearest neighbours rather than aggregate interference only. Note that acquiring such information typically requires more advanced receiver processing or signalling among neighbouring subnetworks. The NNCA will also lead to more complex system design. For instance, dedicated reference sequences need to be designed such that it becomes possible to identify the neighbors.

Note that the fixed channel assignment requires no channel sensing.

2) Centralized Dynamic Channel Group Selection

Although in-X subnetworks are envisioned to be independent subnetworks, there are certain applications where reliable connection to a larger network is possible. In such cases, it may be advantageous to manage radio resources in a centralized manner. Also, a centralized scheme can be used as a benchmark for evaluating the performance of distributed approaches. In [34], centralized graph coloring (CGC) was used for this purpose.

The CGC involve improper coloring of a mutual coupling graph, G_t to assign colors (or equivalently channel group) to all subnetworks. The weighted undirected graph, G_t is

created at time instant, t from the $N \times N$ mutual inter-subnetwork interference matrix, $\mathbf{I}(t)$. While it is possible to create $\mathbf{I}(t)$ using sensing measurements at both the AP and devices, in the following we assume for simplicity that $\mathbf{I}(t)$ contains interference powers measured at the AP in each subnetwork.

In G_t, each vertex corresponds to an in-X subnetwork in the network. Edges are created by connecting each vertex to its $K-1$ nearest neighbours. The weight of each edge is set equal to the interference power between the interfering subnetworks. Assuming that G_t is K-colorable at every time instants, applying greedy coloring on G_t is guaranteed to yield reasonable channel group assignment. Our earlier studies have however shown that the edge creation rule results in few instances for which G_t is not K-colorable.

To guarantee K-colorability of G_t, we propose a graph sparsity constraint procedure which involve successive elimination of the edge with the lowest weight from G_t until it can be colored by at most K colors.

B. ANTICIPATORY PACKET DUPLICATION

In the schemes described above, transmissions within each subnetwork are restricted to a single channel group at a given time instant. Since no coordination is assumed among the different subnetworks, each subnetwork then make decisions on which group to transmit based solely on its own local sensing information. This lack of information about the intention of other subnetworks may result in unanticipated switching of a strong interfering neighbour to the channel currently occupied by another subnetwork translating to a potentially high interference, and hence failed transmissions. To circumvent this problem, we propose a novel procedure referred to as anticipatory packet duplication (APDP). APDP involves duplicating packets on a secondary channel group and is activated when the presence of a potentially harmful neighbouring subnetwork is detected. This duplication allows for increased combining gain and is performed at each subnetwork based on the estimate of an anticipated achieved rate, $\tilde{R}_{apdp}$ obtained from (5). The SINR is calculated with the perceived interference power from the strongest non-colliding neighbour added to the total received interference power. In Algorithm 1, we present a summary of the procedure for performing dynamic channel selection with APDP. This procedure allows each subnetwork to select a primary channel group for transmission using any of the methods described in Section III-A. When the decision to duplicate is made, the AP selects the best from the available channel group list (all groups excluding the current primary group) as the secondary channel group for duplicating packets.

We remark here that the total interference footprint in the system will increase with activation of APDP. However, we expect the combining gain to outweigh this increase depending on the deployment density and subnetwork load.

Algorithm 1 Dynamic Channel Selection with Anticipatory Packet Duplication for Mobile in-X subnetworks

Input: Target rate, R_{target}, available channel groups, G
while active **do**
  Each subnetwork perform primary channel group selection using any of the methods in section III-A
  Assign randomized hopping patterns to all devices
  Perform transmission and measure the worst case SINR on primary channel group
  Measure interference power on all channel groups
  for each subnetwork **do**
    Estimate anticipated SINR using (4) with the interference power from the strongest non-colliding neighbour added to the denominator
    Estimate anticipated worst-case rate $\tilde{R}_{\text{apdp}}$
    if $\tilde{R}_{\text{apdp}} \leq R_{\text{target}}$ **then**
      Select a secondary channel group randomly or as the best group in G that is not in use as the primary group
      Activate APDP
    else
      De-activate APDP
  for each subnetwork **do**
    if minimum achieved rate $\leq R_{\text{target}}$ **then**
      Apply selection rule to update primary channel group
      Perform channel group switching
  Continue transmission

C. REPETITION ORDER ADAPTATION

As stated in Section II, a major MAC feature for satisfying the stringent requirements in 6G in-X subnetworks is blind repetition of packets over multiple frequency channels with energy combining. While such blind repetitions may indeed make the system more robust to interference, it can lead to re-transmissions which are not necessary to correctly decode the packet and hence, low spectral efficiency. To improve the spectral efficiency, we propose an adaptation technique involving adjustment of the number of repetitions based on the experienced SINR level at each device.

Let us define a binary indicator for successful decoding of a packet after the kth repetition is received as

$$\beta(k) = \begin{cases} 1 & \text{if UL and DL packet is correctly decoded} \\ 0 & \text{otherwise} \end{cases}, \tag{1}$$

and denote the number of repetitions used by the mth device in subnetwork n at transmission instant, t and the minimum (maximum) number of repetitions as $P_{nm}(t)$ and P_{min} (P_{max}), respectively. If the transmission at time t is successful, i.e., $\beta(P_{nm}(t)) = 1$, the number of repetitions for the next transmission, dropping the subscript index of P for clarity,

is set as

$$P(t+1) = \begin{cases} P(t) - 1 & \text{if } P(t) \neq P_{\min} \text{ and } \beta(P(t)-1) = 1 \\ P(t) & \text{Otherwise} \end{cases} \quad (2)$$

With a failed transmission at time t, the number of repetitions is set using

$$P(t+1) = \begin{cases} P(t) + 1 & \text{if } P(t) < P_{\max} \\ P(t) & \text{Otherwise.} \end{cases} \quad (3)$$

The adaptation criteria in (2) and (3) ensures that each device only utilize the number of repetitions that is estimated to be necessary for correct decoding of the transmitted packets at any given time instant. This procedure is expected to result in reduced total interference footprint in the network. The unused resources can also be dynamically allocated to other devices leading to more efficient spectrum utilization. Design of enabling protocol for such resource reuse is however left for future work.

IV. EVALUATION PROCEDURE AND MODELS

We evaluate the in-X subnetwork technology and the presented approaches in a simulated factory area with parameters from 3GPP specifications [40]. The models for wireless channel, SINR and rate, scenario and deployment settings, performance metrics and the simulation procedure are presented in this section.

A. SCENARIO AND SETTINGS

We consider an indoor factory setting with $N = 20$ mobile in-X subnetworks as illustrated in Fig. 2. Such subnetworks can for example, be used to wirelessly control the robot arms. Except where stated otherwise, each subnetwork has an AP located at the center of its circular coverage area with 3.0 m radius and $M = 6$ uniformly distributed sensor-actuator pairs. We assume for simplicity that each sensor and its corresponding actuator are co-located. Considering the coverage range of the subnetworks, the transmit power per transmission is set to -10 dBm. We consider a total bandwidth of 1200 MHz which is partitioned into six 200 MHz-channel groups. Transmission within each subnetwork is then performed using a single channel group at any given time. Each group is further partitioned into between 6 and 36 channels. Within each group, transmissions within a subnetwork occur over orthogonal hopping sequences thereby eliminating intra-subnetwork interference. The hopping patterns are generated randomly for each transmission instance following the structure in Fig. 1a. Although, effect of jamming on communication performance is beyond the scope of this paper, the randomization of hopping pattern is expected to provide a tier of resilience to malicious attacks. The total bandwidth and total number of devices are kept constant translating to a fixed system spectral efficiency.

TABLE 3: Simulation parameters. The propagation parameters are selected from [40]. The target rate is calculated assuming that ∼20% of the subcarriers in an OFDM symbol are allocated to reference sequences for channel estimation

Deployment and system parameters				
Parameter	Value			
Factory area [m^2]	40×40			
Number of in-robot subnetworks, N	20			
Number of devices per subnetwork, M	6			
subnetwork radius [m]	3.0			
Velocity, v [m/s]	3.0			
Mobility model	Restricted RDM			
Number of receive antenna	2			
Propagation and radio parameters				
Channel model	3GPP Indoor Factory			
Pathloss exponent, γ	2.55			
Shadowing standard deviation, σ_s [dB]	5.7			
De-correlation distance, d_c [m]	10			
Lowest frequency [GHz]	6			
Transmit power per channel [dBm]	-10			
Noise figure [dB]	10			
Fading block bandwidth [MHz]	10			
Antenna correlation parameter, ζ	0.1			
Simulation settings				
Sampling interval [μs]	100			
Channel group switching delay	[1,8]			
Total bandwidth [MHz]	1200			
Payload size (Bytes)	20			
Number of Groups	6			
Bandwidth per group [MHz]	200			
Bandwidth per channel [MHz]	33,33	16,67	8,33	5,56
Total number of subcarriers	69	35	17	12
Number of data subcarriers	56	28	14	9
Number of subcarriers for reference sequences	13	7	3	3
Target rate	0,71	1,43	2,86	4,44

B. WIRELESS CHANNEL MODEL

The wireless communication channel between the controllers and devices (sensors and actuators) comprises of three components: path-loss, shadowing and small-scale fading which are modeled as follows:

- Path-loss: We consider the 3GPP path-loss model for in-factory environment with sparse clutter and low antenna heights [40].
- Shadowing: A correlated log-normal shadowing model based on a 2D Gaussian random field is considered [41].
- Small-scale fading: The small scale fading, h are modelled as Rayleigh distributed random variables. A block fading model with a coherence bandwidth of 10 MHz is assumed. To model temporal correlation of the small-scale channel, we utilized the Jake's Doppler model [42]. Small-scale fading across multiple frequency channels over which a device hops is assumed to be independent. To capture correlations among receptions at multiple antennas, we consider the one-sided Kronecker model with Toeplitz correlation matrix, $\mathbf{V}$ [43] and define $\mathbf{h} = \mathbf{V}^{1/2}\mathbf{g}$, with $\mathbf{V}(i,j) = \zeta^{|j-i|}; 0 \leq \zeta < 1$ denoting the receive correlation matrix and $\mathbf{g}$ is an iid circular symmetric random vector.

C. SINR AND RATE MODEL

As a result of the lack of coordination, transmissions from different subnetworks are misaligned resulting in potential cross-link interference. Assuming a block fading model, the signal to noise-plus-interference ratio (SINR) on the ℓth

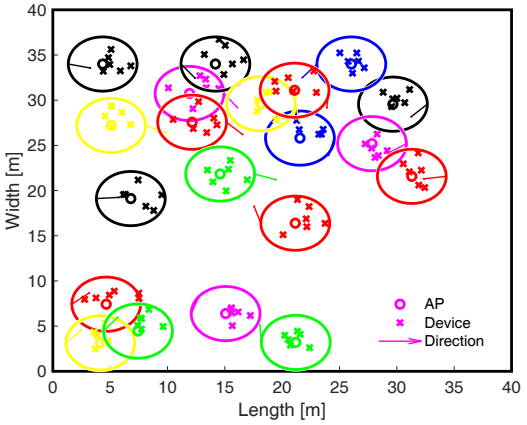

FIGURE 2: A snapshot of the considered deployment with 20 mobile in-X subnetworks, each with 6 devices, operating within an industrial factory hall with minimum inter-subnetwork distance of 3 m. The colors indicate randomly assigned channel group to each cell.

fading block between the AP in subnetwork n and its mth device at time t can be expressed as

$$\rho_{nm}^{\ell z}[t] = \frac{|h_{nm}[t]|^2 Y_{nm}[t]}{\sum_{k\in\mathcal{I}_{nm}} |h_k[t]|^2 Y_k[t] + \sigma_n^2} \tag{4}$$

where $h_{nm}(Y_{nm})$ and $h_k(Y_k)$ denote the small scale fading (received large scale power) on the link between AP n and device m, and the small-scale gain (large scale power for the kth interference source), respectively. The set $\mathcal{I}_{nm}$ denote the set of all devices and APs that are active on the same channel by device m in the nth subnetwork at the same time. $\sigma_n^2 = 10^{(-174+\mathrm{NF}+10\log_{10}(\mathrm{BW}))/10}$ is the noise power with NF and BW denoting the noise figure and bandwidth per fading block, respectively.

Considering chase combining of the P packet repetitions over Z receive antennas, the achieved rate on a link between device m and the nth AP can be expressed as

$$R_{nm}[t] = \frac{1}{L}\sum_{\ell=1}^{L} \log_2\left(1 + \sum_{z=1}^{Z}\sum_{p=1}^{P} \rho_{nm}^{\ell z}[p,t]\right), \tag{5}$$

where L denotes the number of fading blocks. The SINR threshold, ρ_{th} is determined as the minimum SINR value for which the rate in (5) is above the target rate. Assuming a packet of B bytes is mapped over the entire channel bandwidth, the target rate is calculated as $R_{\text{target}} = 8B/(N_{\text{ofdm}}N_{\text{data}})$, where N_{ofdm} and N_{data} denote the number of OFDM symbols and number of data subcarriers per symbol, respectively.

D. PERFORMANCE METRICS

Three key performance metrics viz: latency, communication system reliability (CSR) and survival time, τ_{surv} are considered in the evaluation. Relying on the frame structure in Fig. 1a in which the cycle time (i.e., the total time between transmission of data from the sensor to the processing of associated command from the controller to the actuator) is set by design to a maximum of 100 μs, we conclude that the latency requirement is always satisfied. We measure the communication system reliability using the Packet Loss Rate (PLR) defined as the probability that no successful packet reception occurs within a continuous period that is less or equal to τ_{surv}. Notice that while certain critical applications may not tolerate any packet loss, others which are more relaxed may be able to survive without specific number of packets. For example, the work in [44] indicated that remote control of harbor cranes exhibit survival times as large as six consecutive packet transmissions. We therefore concentrate on evaluating the relationship between PLR and τ_{surv} with the in-X subnetworks enablers and the different mechanisms described above.

E. SIMULATION PROCEDURE

A snapshot based simulation technique in which performance metrics are measured over multiple snapshots is developed and used for this evaluation. The simulation involves:

1) **Deployment generation:** Within each snapshot, the layout is created by deploying the controllers (i.e., APs) on the factory floor following a uniform distribution. With each AP's location as the center, devices are distributed uniformly within a circular coverage area of the subnetwork with radius, r_{sub}.
2) **Mobility pattern generation**: Following a restricted random direction model (RDM), the in-X subnetworks move with constant speed, v for the entire snapshot duration, τ_{snap}. The location of all subnetworks and associated devices are then collected at every transmission interval. To avoid unrealistic collision of subnetworks, each subnetwork randomly changes movement direction if its distance to any other subnetwork is less than a specified minimum inter-subnetwork distance, d_{min}. A random direction change is also performed if the distance between a subnetwork and any of the factory walls at the next time instant is estimated to be less than its coverage radius.
3) **Fading channel generation:** Based on the models and assumptions presented in section IV-B, correlated small- and large-scale (path-loss and shadowing) fading are computed over the snapshot.
4) **Channel Assignment:** Each subnetwork selects a channel group randomly at the beginning of each snapshot or using any of the dynamic channel allocation schemes in section III-A. Given a predefined frame structure, devices in each subnetwork are allocated orthogonal channels per each transmission instant, including repetitions. The channel hopping pattern is different at each subnetwork. This is meant to randomize the interference and avoid a situation where a device is persistently interfered over multiple repetitions by the same devices.
5) **Power, SINR and Rate computation:** The received signal power and interference power are calculated at

each transmission instant using the path-loss models defined in [40]. The SINR and achieved rate on both links of each loop are then calculated using (4) and (5), respectively.

6) **PLR calculation:** For a given survival time, τ_{surv} (in number of cycles), the PLR is calculated as the probability that the achieved rate on either or both the UL and DL of a loop is less than the target rate, R_{target} over a number of successive transmission cycles that is less than or equal to τ_{surv}.

The PLR for a given τ_{surv} is computed as

$$\text{PLR}[\tau_{\text{surv}}] = \frac{1}{NMS}\sum_{n=1}^{N}\sum_{m=1}^{M}\sum_{s=1}^{S}\Pr[R^{s}_{nm}[\tau_{\text{surv}}] < R_{\text{target}}], \tag{6}$$

where S denotes the number of snapshots and $R^{s}_{nm}[\tau_{\text{surv}}]$ is the maximum achieved rate by device m in subnetwork n over any consecutive transmission with duration of τ_{surv} in the sth snapshot.

It should be noted that the rate expression in (5) and hence, the PLR calculation in (6) relies on the assumption of capacity-achieving codes. However, commonly used codes have been shown to approach such capacity only with large block-lengths [45], [46], which may clearly not be the case for the short packets in 6G in-X subnetworks. Nonetheless, using capacity-achieving codes eliminate the need of making specific assumptions on the actual channel coding technique for 6G in-X subnetworks, which is currently not defined. Also, the assumption of perfect channel state information (CSI) at the receiver for the PLR calculation in (6) is overly optimistic since CSI for coherent detection is typically estimated from reference signals, and in practice making deviations from the ideal CSI inevitable [47], [48]. Moreover, the target rate, R_{target} may exhibit spatio-temporal variations due to the dynamic nature of the environment. The target rate should therefore be dynamically estimated using for example, the statistical learning methods in [49]. The results presented in this paper can therefore be seen as optimistic bounds, and potential deviations may occur in case realistic channel coding techniques with finite block-length, more realistic rate estimates and non-idealized channel estimation models are available. These aspects are left for future studies.

V. PERFORMANCE RESULTS

We study the PLR - survival time relationship for the different techniques presented in Section III using the numerologies in Table 2 and the simulation parameters in Table 3. The goal is to understand how well the different techniques can support the latency and PLR requirements for in-X subnetworks operating in typical industrial environments. To guarantee high statistical significance of the results, we evaluate the performance metrics over about $1.2\times10^{10}(500\times2\times10^{5}\times20\times6)$ samples corresponding to 500 snapshots each with 2×10^{5} samples per device. For clarity, the results are presented in three sections viz: (A) fixed channel group assignment in which channel groups are randomly selected at the beginning of each snapshot and kept for the entire snapshot duration; (B) in-X subnetworks with environment-aware dynamic channel group selection methods and (C) in-X subnetworks with environment aware selection and repetition order adaptation or anticipatory packet duplication.

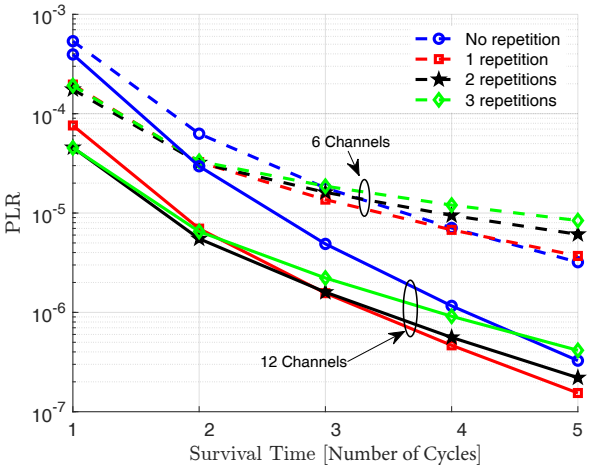

FIGURE 3: PLR versus survival time with fixed channel group assignment and varying repetition order.

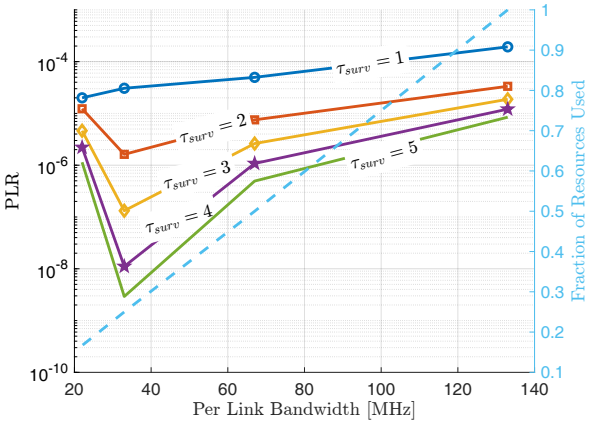

FIGURE 4: PLR versus per link bandwidth with fixed assignment (left y-axis) and fraction of resource used (right y-axis).

A. PERFORMANCE WITH FIXED CHANNEL GROUP ASSIGNMENT

Fig. 3 shows the PLR as a function of survival time with 6 and 12 channels over each 200 MHz channel group and number of repetitions between 0 and 3. Note that having 12 channels lead to a lower channel bandwidth of 16.67 MHz relative to 6 channels with 33.33 MHz. A single transmission will then be mapped over a smaller bandwidth and therefore have a larger transmission rate; on the other side, interference will be more sparse in the case of 12 channels as there are more opportunities for channel hopping.

In case, the system can tolerate no failures (i.e., with a survival time equal to 1 cycle duration of $\sim$ 86μs), the PLR decreases with increasing number of repetitions, thanks to the combining gain. For both number of channels, no

noticeable decrease in PLR at $\tau_{\text{surv}} = 1$ is obtained beyond 2 repetitions, or equivalently a total of 3 transmissions. The figure further shows that the gain from packet repetitions diminishes with increased survival time. For instance, while the lowest PLR with 6 channels is obtained with a single repetition at $\tau_{\text{surv}} = 2$, no repetition is required for the best performance at $\tau_{\text{surv}} = 5$. Notice that further increase in number of repetitions leads to an increase in PLR with high survival time (i.e., $\tau_{\text{surv}} \geq 3$). A plausible explanation for this is the increase in interference level in the network associated with increasing repetitions. It is therefore crucial to accurately set the number of repetitions to avoid performance degradation. Fig. 3 also shows that it is more advantageous to have narrower channels and consequently, lower probability of collision on each channel than having fewer channels with large bandwidth. It is however expected that there is a limit on how narrow the channel bandwidth can be in order to support the target rate.

To understand the trade-off between channel bandwidth and resource utilization, we plot the PLR as a function of per link bandwidth (i.e., product of the bandwidth per channel and the number of packet repetitions per link) as well as the corresponding fraction of resources used in Fig. 4. The figure shows that the PLR increases with increasing per link bandwidth (and correspondingly increasing resource utilization) except for cases with $\tau_{\text{surv}} > 1$ which exhibit an initial sharp decrease in PLR. In general, the figure indicates that increasing the link bandwidth leads to higher utilization of resources and therefore higher interference level, which in turn results in worse PLR in spite of the more robust coding due to the larger bandwidth per channel. For the considered scenario, having a relatively small per link bandwidth (approximately 34 MHz) and low resource utilization (about 22%) appear to be optimal.

B. BENEFIT OF ENVIRONMENT-AWARE MECHANISMS

As shown in Fig. 3 and Fig. 4, for in-X applications with survival time, $\tau_{\text{surv}} = 1$ (i.e., systems that tolerate no packet loss), interference diversity via blind repetition with random hopping pattern alone is not sufficient to satisfy the below 10^{-6} PLR requirement within the $\leq$ 100 μs latency. This shows that environment-aware interference coordination is inevitable in order to support the requirements for in-X subnetworks.

In Fig. 5, we show the achieved PLR with the dynamic channel allocation schemes described in section III-A. Similar to Fig. 3, we show the PLR versus survival time with 6 and 12 channels per group. As expected, the environment aware algorithms lead to a significant PLR reduction in both cases. Due to the reduction in probability of interference from lower resource utilization, having 12 channels shows slightly better performance than with 6 channels. The reduction in PLR is dependent on the survival times, varying from a factor of $\sim 10^2$ at $\tau_{surv} = 1$ to about 10^5 at $\tau_{surv} = 4$. Compared to the distributed schemes (i.e., Greedy and NNCA) which has similar performance, the CGC shows marginally lower

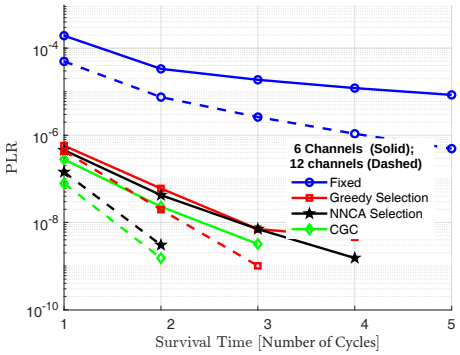

FIGURE 5: PLR versus survival time with environment aware interference coordination.

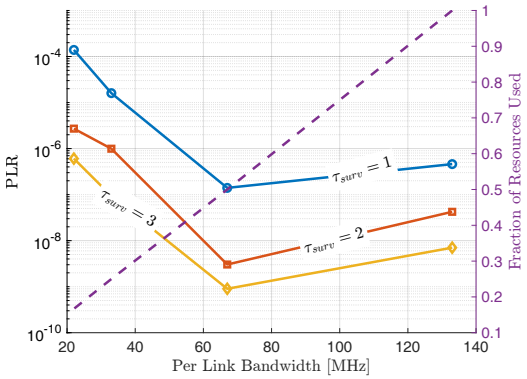

FIGURE 6: PLR versus per link bandwidth with varying survival time and environment aware interference coordination.

PLR.

Fig. 6 shows the PLR versus per link bandwidth relationship and the equivalent resource utilization with NNCA selection. Compared to the results in Fig. 4, the figure shows that relatively larger per link bandwidth ($\sim$ 68 MHz) with higher resource utilization ($\sim$ 50%) gives the best PLR performance for in-X subnetworks utilizing environment-aware coordination schemes. This indicates that increasing the resource utilization beyond $\sim$ 50% is not beneficial for the PLR. A plausible explanation for this is that increased resource utilization leads to higher interference which turns out to be detrimental for the performance. On the other side, if resource utilization is too small, i.e., small channels are used, performance are still unsatisfactory. This is expected since interference becomes rather sparse with low resource utilization, making the impact of fading and hence, channel bandwidth on the PLR more pronounced.

C. PLR PERFORMANCE WITH ENHANCEMENT MECHANISMS

We now evaluate the benefits of adaptive repetition order and anticipatory packet duplication on the achieved PLR.

Fig. 7 shows the PLR versus survival time with fixed channel group assignment and the greedy channel selection scheme. We consider cases with a fixed repetition order, i.e., $P = 4$ corresponding to a total of 3 repetitions and adaptive

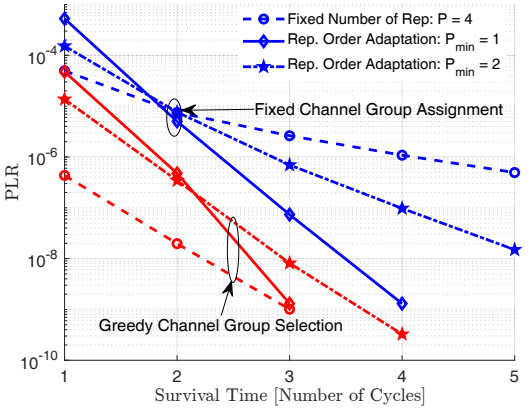

FIGURE 7: PLR versus survival time with repetition order adaptation.

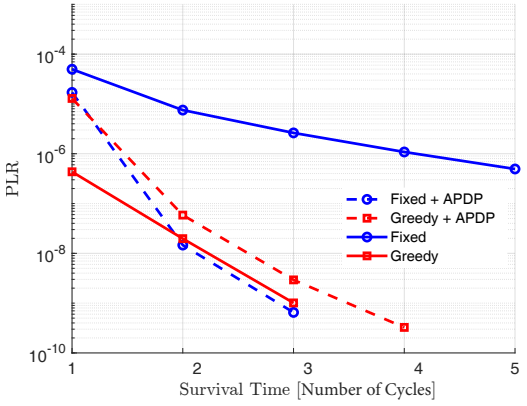

FIGURE 8: PLR versus survival time with anticipatory packet duplication (APDP). The averaged APDP activation rate for the random and greedy schemes are: 1.02×10^{-4} and 7.73×10^{-5}.

repetition order with the minimum number of transmissions equals to 1 and 2. The results indicate that adaptation of repetition order offers significant PLR reduction with $\tau_{\text{surv}} \geq 2$. The performance improvement is however dependent on the presence or otherwise of environment-aware schemes and the minimum number of transmissions, P_{min}. For example, the PLR reduction at $\tau_{\text{surv}} = 4$ with fixed channel assignment is significantly larger for $P_{\text{min}} = 1$ ($\sim 10^3$) than for $P_{\text{min}} = 2$ (~ 10). The degradation in performance with repetition order adaptation at $\tau_{\text{surv}} = 1$ is potentially due to the non-proactive nature of the procedure in section III-C in which decisions for the number of repetitions for the next slot is made based solely on knowledge at the current slot.

Finally, we illustrate the effect of APDP on achieved PLR in Fig. 8. We consider both fixed and greedy channel group selection with and without APDP. For both schemes, greedy selection is applied to choose the secondary group when decision to activate duplication is made. The figure shows that packet duplication leads to a degradation in the performance of the environment-aware channel selection (i.e., greedy). An indication that the effect of increased interference outweighs the combining gain from duplication in scenarios where interference on the primary group is coordinated. In contrast, APDP results in huge reduction in PLR (up to a factor of 10^3 at $\tau_{\text{surv}} = 3$) with fixed primary group assignment. It should however be noted that the best performance with APDP is similar to that of greedy without APDP and that APPD requires simultaneous transmission over more than one channel group in addition to channel sensing, leading to a potential complexity increase. For example, more than one transceiver chain are needed for simultaneous transmission and reception in 2 channel groups.

D. COMPUTATIONAL COMPLEXITY

We now analyze the computational complexity of the environment aware schemes for DDCGS, i.e., greedy selection and NNCA as well as the enhancement mechanisms - adaptive repetition order and APDP. We estimate the complexity by counting the total number of operations for each method. Note that each method includes three steps viz: sensing, decision and switching or adaptation. The third step involves either a single ± 1 operation on the number of repetitions or simply jumping to a new channel group, resulting in a $\mathcal{T}(N)$ number of operations for all methods. Since all methods require similar sensing measurements, we consider a fixed computation cost for the sensing step of all schemes. This is reasonable since the actual cost associated with this step depends on the sensing capabilities of the access points and not on the interference management methods. Note that the NNCA scheme may incur an additional cost due to the required information about the channel occupied by the strongest interfering subnetworks. This is however ignored in the analysis. For the greedy channel group selection only an argmax operation is performed on the $K \times 1$ interference power vector, translating to a total of $K - 1$ comparison operations per subnetwork at each time step. The total complexity for the decision step of the greedy scheme is therefore given by $\mathcal{T}((K-1)NS_t)$, where S_t denotes the number of steps over all snapshots. The NNCA scheme instead involve comparison of two sets - a set of the channel groups occupied by $K-1$ strongest interfering neighbours and a set of all K channel groups. This requires a maximum of $K(K-1)$ comparisons to make channel group selection per subnetwork at a given time step, leading to a total complexity of $\mathcal{T}(K(K-1)NS_t)$ over all snapshots. Following a similar procedure, the complexity of APDP and adaptive repetition order selection are obtained as shown in Table 4. As shown in the table, the computational complexity of greedy selection, NNCA and APDP grows linearly with the number of subnetworks, N and the total number of time steps, S_t. For adaptive repetition order, the complexity grows linearly with the total number of devices, MN and S_t. In the asymptotic limits of large number of subnetworks, N and number of time steps, S_t, the number of available channel groups, K becomes much less than N and S_t, i.e., $K << N$ and $k << S_t$. Assuming that $M << N$, the asymptotic

	Greedy	**NNCA**	**APDP**	**Adaptive Repetition Order**
Sensing	$\mathcal{T}(NS_t)$	$\mathcal{T}(NS_t)$	$\mathcal{T}(NS_t)$	$\mathcal{T}(S_t)$
Decision	$\mathcal{T}((K-1)NS_t)$	$\mathcal{T}(K(K-1)NS_t)$	$\mathcal{T}((K-1)NS_t)$	$\mathcal{T}(M)$
Switching	$\mathcal{T}(NS_t)$	$\mathcal{T}(NS_t)$	$\mathcal{T}(NS_t)$	NA
Adaptation	NA	NA	NA	$\mathcal{T}(NMS_t)$
Total	$\mathcal{T}((K+1)NS_t+1)$	$\mathcal{T}((K^2-K+2)NS_t)$	$\mathcal{T}((K+1)NS_t)$	$\mathcal{T}((NM+1)S_t+M)$
Asymptotic complexity	$\mathcal{O}(NS_t)$	$\mathcal{O}(NS_t)$	$\mathcal{O}(NS_t)$	$\mathcal{O}(NS_t)$

TABLE 4: Computational complexity of environment aware distributed channel group selection and enhancement schemes

complexity of all methods can be obtained from the total operation count in Table 4 to be $\mathcal{O}(NS_t)$.

VI. DISCUSSION

In our analysis, we saw that the presented radio concepts for in-X subnetworks combined with appropriate environment-aware interference coordination techniques can support the below 10^{-6} error probability within the required latency of 100 μs. However reasonably large bandwidth, blind packet repetitions and interference coordination are important for obtaining such low error probability. As mentioned earlier, there may be a deviation in the evaluation results if non-ideal channel estimation [47], [48] and more realistic channel coding with finite blocklengths [45], [46] are considered. However, changes in the relative performance trends are expected to be insignificant. We remark that although we have not addressed channel estimation issues in this paper, in the rate calculations for our simulations we have assumed that 20% of the subcarriers in an OFDM symbol are allocated to reference sequences for channel estimation. Each transmission carries then these reference sequences in an OFDM symbol, whose duration is 2.15 μs. Such time is significantly shorter than the expected coherence time of the channel at the considered speed of 3 m/s, and therefore no significance channel estimation performance variation due to mobility is expected.

Blind repetitions with frequency hopping focuses on exploiting interference diversity across multiple repetitions of the same packet by applying appropriate receiver processing, e.g., energy combining, on the received packet replica. The presented results as well as findings from our prior studies [29], [34] have indeed shown that re-transmission of the same packets over multiple frequency channels is crucial for extreme communication. As a result of the tight latency requirement, blind repetitions appears to be the only visible option for in-X subnetworks despite its obvious limitations in terms of redundancy compared to Automatic Repeat Request (ARQ) type of retransmission. Our results have indicated that the number of required packet repetitions depends strongly on the survival time. For instance, we observed that a single packet repetition result in $\sim$ $10\times$ and $\sim$ $4\times$ reduction in packet loss rate with survival times of 1 and 4 cycle times, respectively. We saw that further increase in the number of repetitions above 2 degrades the performance. The degradation also increases with increasing survival time. In general, the analysis indicated a maximum of 2 repetitions for systems with $\tau_{\text{surv}} \leq 2$ and a single repetition with more relaxed survival times. As stated earlier, in-X subnetworks are expected to support extreme communication with $\leq 10^{-6}$ outage probability. With the system settings (total bandwidth, number of receive antennas and number of repetitions) considered in our simulations, this extreme requirement appear impossible for in-X subnetwork relying only on the combining gain from blind repetitions to mitigate interference. This is particularly true for operations where the tolerated number of consecutive losses is less than 3.

On the other hand, the environment-aware interference coordination methods (i.e, greedy, NNCA and CGC) target reduction of the interference level by limiting re-use of channel groups to distant subnetworks. This has been shown to yield up to $100\times$ reduction in PLR even for the most critical services, i.e., services with survival time equal to the cycle time of 100 μs. It is therefore reasonable to infer that the extreme requirements for in-X subnetworks can only be guaranteed with efficient interference coordination. Fortunately, the methods presented in this paper are simple both from a design and implementation perspective. For example, the only requirement by the simplest scheme, i.e., greedy channel group selection is sensing of aggregate interference power which can be achieved even with low cost receivers.

Our analysis have further highlighted the combined effects of fading (including small scale fading, pathloss and shadowing) and interference on the achievable PLR performance in dense in-X subnetworks. Designs for in-X subnetworks should therefore incorporate careful trade-off analysis between mechanisms offering robustness to fading and those intended for interference mitigation. For example, results indicated that increased fading-resilience achieved with larger bandwidth per packet transmission leads to reduced loss rate only in scenarios where environment aware schemes are utilized. This is expected since having larger bandwidth per transmission leads to lower number of channels and hence, increased probability of collision on each channel.

The proposed enhancement mechanisms - APDP and repetition order adaptation appear promising only for in-X subnetworks with survival time above 2 cycle times. Such adaptations should therefore be avoided for subnetworks supporting applications for which no packet loss is tolerated. Note that this limitation may be due to the non-proactive nature of the methods. For instance, estimate of the number

of required repetitions for the next transmission is based only on current channel conditions without any account for potential changes due to the highly dynamic in-X subnetwork environment. Despite the limited performance gain, we believe these methods form useful basis for the design of more pro-active and/or intelligent techniques aimed at enhancing resilience of in-X subnetworks to interference.

The combination of MAC and RRM features presented in this paper appear to provide in-X subnetworks operating in industrial scenarios with sufficient resilience to interference leading to PLR lower than the 10^{-6} target. In the case of in-X subnetworks operating in other envisioned scenarios such as in-vehicle or in-human body, the methods presented here may require modifications and/or redesign. For instance, the simple heuristic algorithms (e.g., greedy) for performing implicit interference coordination will require proactive mechanisms such as prediction of future interference power in in-vehicle scenarios where the fast vehicular mobility may quickly lead to aged sensing measurements and hence, erroneous channel group selection decisions. Fortunately, the presented methods allow for easy incorporation of other enhancements. As an example, the greedy selection rules can be easily applied to predicted interference power leading to possible performance improvement.

Although the analysis presented in this paper is based on 3GPP channel models and propagation parameters for industrial environments, the results only give an indication of the expected performance and trade-offs (e.g., increased fading-resilience from large bandwidth per transmission versus reduced interference), and do not guarantee absolute limits on the evaluated metrics in actual 6G in-X subnetworks scenarios. An interesting avenue for future works is indeed to characterize representative in-X operational environments and compare with the 3GPP models used in this paper. Such characterization is then expected to lead to a fully realistic assessment of the performance of in-X subnetworks in dense scenarios.

VII. CONCLUSION

Support for extreme requirements in mobile 6G in-X subnetworks requires a combination of relatively large bandwidth ($\geq$ 1 GHz), interference-robust MAC design, and appropriate interference coordination mechanisms. In this paper, interference-resilient radio design for supporting extreme connectivity as well as mechanisms for mitigating inter-subnetwork interference is presented. Extensive simulation results in typical industrial factory environments have indeed shown that with total bandwidth of 1200 MHz, the below 10^{-6} error probability can be achieved for systems with survival time equal to the cycle time (i.e., systems tolerating no packet loss) by combining up to 2 blind packet repetitions, frequency hopping and environment-aware dynamic channel allocation. The gain from packet repetitions, however, diminishes with increasing survival times indicating that systems that tolerate large number of packet losses can survive with a single packet repetition. Adaptation of repetition order is beneficial for systems with survival time greater than or equal to twice the cycle duration but requires more proactive or predictive mechanisms in case the system allows for no packet loss. While the combining gain from duplicating packets on multiple channel groups may appear promising for reducing packet losses, it should be avoided in scenarios where interference is coordinated.

ABBREVIATIONS

The following abbreviations are used in this manuscript:

5G	5th Generation
6G	6th Generation
in-X	inside everything
B5G	Beyond 5th Generation
3GPP	3rd Generation Partnership Project
4G	4th Generation
URLLC	Ultra-reliable Low Latency Communication
PROFIBUS	Process Fieldbus
FIP	Factory Instrumentation Protocol
P-Net	P-Net field bus standard
HART	Highway Addressable Remote Transducer
WIA	Wireless networks for Industrial Automation
FA	Factory Automation
WISA	Wireless Interface for Sensors and Actuators
RT-WiFi	Real Time Wireless Fidelity
PLR	Packet Loss Rate
DCA	Dynamic Channel Allocation
APDP	Anticipatory Packet Duplication
QoS	Quality of Service
OFDM	Orthogonal Frequency Division Multiplexing
AP	Access Point
UL	Uplink
DL	Downlink
PHY	Physical layer
CP	Cyclic Prefix
TDD	Time Division Duplexing
FDD	Frequency Division Duplexing
MAC	Medium Access Control
RRM	Radio Resource Management
DCGS	Dynamic Channel Group Selection
DDCGS	Distributed Dynamic Channel Group Selection
SINR	Signal-to-Interference - plus - Noise Ratio
NNCA	Nearest Neighbour Conflict Avoidance
CGC	Centralized Graph Coloring
NF	Noise Figure
CSR	Communication System Reliability
RDM	Random Direction Model
ARQ	Automatic Repeat Request
EtherCAT	Ethernet for Control Automation Technology
ISA	International Society of Automation
IEEE	Institute of Electrical and Electronics Engineers
MEC	Mobile Edge Computing
CSI	Channel State Information

REFERENCES

[1] J. R. Moyne and D. M. Tilbury, "The emergence of industrial control networks for manufacturing control, diagnostics, and safety data," Proceedings of the IEEE, vol. 95, no. 1, pp. 29–47, 2007.

[2] B. Galloway and G. P. Hancke, "Introduction to industrial control networks," IEEE Communications Surveys Tutorials, vol. 15, no. 2, pp. 860–880, 2013.

[3] A. Aijaz, "High-performance industrial wireless: Achieving reliable and deterministic connectivity over ieee 802.11 wlans," IEEE Open Journal of the Industrial Electronics Society, vol. 1, pp. 28–37, 2020.

[4] M. Luvisotto, Z. Pang, and D. Dzung, "High-performance wireless networks for industrial control applications: New targets and feasibility," Proceedings of the IEEE, vol. 107, no. 6, pp. 1074–1093, 2019.

[5] A. Willig, K. Matheus, and A. Wolisz, "Wireless technology in industrial networks," Proceedings of the IEEE, vol. 93, no. 6, pp. 1130–1151, 2005.

[6] W. Liu, Z. Liu, C. Gu, and H. Zhao, "Study of channel adaptive hopping technology on industrial wireless networks," in 2012 Fifth International Symposium on Computational Intelligence and Design, vol. 1, 2012, pp. 62–64.

[7] Y.-t. Ye and H.-d. Lei, "Wireless industrial communication system based on Profibus-DP and ZigBee," in 2016 11th International Conference on Computer Science Education (ICCSE), 2016, pp. 666–669.

[8] W. Liang, M. Zheng, J. Zhang, H. Shi, H. Yu, Y. Yang, S. Liu, W. Yang, and X. Zhao, "WIA-FA and Its Applications to Digital Factory: A Wireless Network Solution for Factory Automation," Proceedings of the IEEE, vol. 107, no. 6, pp. 1053–1073, 2019.

[9] Q. Chen, X. J. Zhang, W. L. Lim, Y. S. Kwok, and S. Sun, "High reliability, low latency and cost effective network planning for industrial wireless mesh networks," IEEE/ACM Transactions on Networking, vol. 27, no. 6, pp. 2354–2362, 2019.

[10] O. Seijo, J. A. Lopez-Fernandez, and I. Val, "w-SHARP: Implementation of a High-Performance Wireless Time-Sensitive Network for Low Latency and Ultra-low Cycle Time Industrial Applications," IEEE Transactions on Industrial Informatics, vol. 17, no. 5, pp. 3651–3662, 2021.

[11] L. Chen, S. Yang, and Y. Xi, "Based on ZigBee wireless sensor network the monitoring system design for chemical production process toxic and harmful gas," in 2010 International Conference on Computer, Mechatronics, Control and Electronic Engineering, vol. 4. IEEE, 2010, pp. 425–428.

[12] J. Song, S. Han, A. Mok, D. Chen, M. Lucas, M. Nixon, and W. Pratt, "Wirelesshart: Applying wireless technology in real-time industrial process control," in 2008 IEEE Real-Time and Embedded Technology and Applications Symposium. IEEE, 2008, pp. 377–386.

[13] M. S. Costa and J. Amaral, "Analysis of wireless industrial automation standards: Isa-100.11 a and wirelesshart," InTech Magazine, 2012.

[14] "IEEE Standard for Low-Rate Wireless Networks," IEEE Std 802.15.4-2020 (Revision of IEEE Std 802.15.4-2015), pp. 1–800, 2020.

[15] V. Saravanan, S. Arivoli, and K. Valarmathi, "ZigBee based monitoring and control of melter process in sugar industry," in 2014 International Conference on Electronics and Communication Systems (ICECS), 2014, pp. 1–4.

[16] J. Endresen, "Introduction to WISA," 2006.

[17] Y.-H. Wei, Q. Leng, S. Han, A. K. Mok, W. Zhang, and M. Tomizuka, "RT-WiFi: Real-Time High-Speed Communication Protocol for Wireless Cyber-Physical Control Applications," in 2013 IEEE 34th Real-Time Systems Symposium, 2013, pp. 140–149.

[18] A. A. Esswie and K. I. Pedersen, "Analysis of Outage Latency and Throughput Performance in Industrial Factory 5G TDD Deployments," in 2021 IEEE 93rd Vehicular Technology Conference (VTC2021-Spring), 2021, pp. 1–6.

[19] F. Hamidi-Sepehr, M. Sajadieh, S. Panteleev, T. Islam, I. Karls, D. Chatterjee, and J. Ansari, "5G URLLC: Evolution of High-Performance Wireless Networking for Industrial Automation," IEEE Communications Standards Magazine, vol. 5, no. 2, pp. 132–140, 2021.

[20] H. Viswanathan and P. E. Mogensen, "Communications in the 6G Era," IEEE Access, vol. 8, pp. 57 063–57 074, 2020.

[21] H. Tataria, M. Shafi, A. F. Molisch, M. Dohler, H. Sjöland, and F. Tufvesson, "6G Wireless Systems: Vision, Requirements, Challenges, Insights, and Opportunities," Proceedings of the IEEE, vol. 109, no. 7, pp. 1166–1199, 2021.

[22] W. Jiang, B. Han, M. A. Habibi, and H. D. Schotten, "The Road Towards 6G: A Comprehensive Survey," IEEE Open Journal of the Communications Society, vol. 2, pp. 334–366, 2021.

[23] I. F. Akyildiz, A. Kak, and S. Nie, "6G and Beyond: The Future of Wireless Communications Systems," IEEE Access, vol. 8, pp. 133 995–134 030, 2020.

[24] Y. Sun, J. Liu, J. Wang, Y. Cao, and N. Kato, "When Machine Learning Meets Privacy in 6G: A Survey," IEEE Communications Surveys Tutorials, vol. 22, no. 4, pp. 2694–2724, 2020.

[25] K. B. Letaief, W. Chen, Y. Shi, J. Zhang, and Y. A. Zhang, "The Roadmap to 6G: AI Empowered Wireless Networks," IEEE Communications Magazine, vol. 57, no. 8, pp. 84–90, 2019.

[26] V. Ziegler, H. Viswanathan, H. Flinck, M. Hoffmann, V. Räisänen, and K. Hätönen, "6G Architecture to Connect the Worlds," IEEE Access, vol. 8, pp. 173 508–173 520, 2020.

[27] J. R. Bhat and S. A. Alqahtani, "6G Ecosystem: Current Status and Future Perspective," IEEE Access, vol. 9, pp. 43 134–43 167, 2021.

[28] Y. L. Lee, D. Qin, L.-C. Wang, and G. H. Sim, "6G Massive Radio Access Networks: Key Applications, Requirements and Challenges," IEEE Open Journal of Vehicular Technology, vol. 2, pp. 54–66, 2021.

[29] R. Adeogun, G. Berardinelli, P. E. Mogensen, I. Rodriguez, and M. Razzaghpour, "Towards 6G in-X Subnetworks With Sub-Millisecond Communication Cycles and Extreme Reliability," IEEE Access, vol. 8, pp. 110 172–110 188, 2020.

[30] G. Berardinelli, P. Mogensen, and R. O. Adeogun, "6G subnetworks for Life-Critical Communication," in 2nd 6G Wireless Summit (6G SUMMIT), 2020, pp. 1–5.

[31] G. Berardinelli, N. H. Mahmood, I. Rodriguez, and P. Mogensen, "Beyond 5G Wireless IRT for Industry 4.0: Design Principles and Spectrum Aspects," in 2018 IEEE Globecom Workshops (GC Wkshps), 2018, pp. 1–6.

[32] G. Berardinelli, P. Baracca, R. Adeogun, S. Khosravirad, F. Schaich, K. Upadhya, D. Li, T. B. Tao, H. Viswanathan, and P. E. Mogensen, "Extreme Communication in 6G: Vision and Challenges for 'in-X' Subnetworks," IEEE OJCOM, 2021.

[33] L. Nadeem, M. A. Azam, Y. Amin, M. A. Al-Ghamdi, K. K. Chai, M. F. N. Khan, and M. A. Khan, "Integration of d2d, network slicing, and mec in 5g cellular networks: Survey and challenges," IEEE Access, vol. 9, pp. 37 590–37 612, 2021.

[34] R. Adeogun, G. Berardinelli, I. Rodriguez, and P. E. Mogensen, "Distributed Dynamic Channel Allocation in 6G in-X Subnetworks for Industrial Automation," in IEEE Globecom Workshops, 2020.

[35] R. Adeogun, G. Berardinelli, and P. Mogensen, "Learning to Dynamically Allocate Radio Resources in Mobile 6G in-X Subnetworks," in 2021 IEEE 32nd Annual International Symposium on Personal, Indoor and Mobile Radio Communications (PIMRC), 2021, pp. 959–965.

[36] "Service requirements for cyber-physical control applications in vertical domains; stage 1," 3rd Generation Partnership Project, Tech. Rep. 22.104 v17.4.0, Sep. 2020.

[37] O. Tirkkonen, S. R. Khosravirad, P. Baracca, L. Zhou, U. Parts, D. Korpi, and M. A. Uusitalo, "Optimized Survival Mode to Guarantee QoS for Time-critical Services," in 2021 IEEE International Conference on Communications Workshops (ICC Workshops), 2021, pp. 1–6.

[38] M. Razzaghpour, R. Adeogun, G. Berardinelli, M. Ramsmus, P. Troels, M. Preben, and S. Troels, "Short-Range UWB Wireless Channel Measurement in Industrial Environments," in WIMOB, 2019.

[39] P. W. C. Chan, E. S. Lo, R. R. Wang, E. K. S. Au, V. K. N. Lau, R. S. Cheng, W. H. Mow, R. D. Murch, and K. B. Letaief, "The evolution path of 4G networks: FDD or TDD?" IEEE Communications Magazine, vol. 44, no. 12, pp. 42–50, 2006.

[40] "Study on channel model for frequencies from 0.5 to 100 GHz (Release 16)," 3rd Generation Partnership Project, Tech. Rep. 38.901 v16.1.0, January 2020.

[41] S. Lu, J. May, and R. J. Haines, "Effects of correlated shadowing modeling on performance evaluation of wireless sensor networks," in IEEE Vehicular Technology Conference, 2015, pp. 1–5.

[42] W. C. Jakes and D. C. Cox, Microwave mobile communications. Wiley-IEEE press, 1994.

[43] M. Chiani, M. Win, and A. Zanella, "On the capacity of spatially correlated mimo rayleigh-fading channels," IEEE Transactions on Information Theory, vol. 49, no. 10, pp. 2363–2371, 2003.

[44] H. Kokkoniemi-Tarkkanen, S. Horsmanheimo, A. Grudnitsky, M. Moisio, Z. Li, M. A. Uusitalo, D. Samardzija, T. Härkönen, and P. Yli-Paunu, "Enabling Safe Wireless Harbor Automation via 5G URLLC," in 2019 IEEE 2nd 5G World Forum (5GWF), 2019, pp. 403–408.

[45] Y. Polyanskiy, H. V. Poor, and S. Verdu, "Channel coding rate in the finite blocklength regime," IEEE Transactions on Information Theory, vol. 56, no. 5, pp. 2307–2359, 2010.
[46] W. Yang, G. Durisi, T. Koch, and Y. Polyanskiy, "Quasi-static multiple-antenna fading channels at finite blocklength," IEEE Transactions on Information Theory, vol. 60, no. 7, pp. 4232–4265, 2014.
[47] J. Zeng, T. Lv, R. P. Liu, X. Su, Y. J. Guo, and N. C. Beaulieu, "Enabling ultrareliable and low-latency communications under shadow fading by massive mu-mimo," IEEE Internet of Things Journal, vol. 7, no. 1, pp. 234–246, 2020.
[48] H. Ren, C. Pan, Y. Deng, M. Elkashlan, and A. Nallanathan, "Joint pilot and payload power allocation for massive-mimo-enabled urllc iiot networks," IEEE Journal on Selected Areas in Communications, vol. 38, no. 5, pp. 816–830, 2020.
[49] M. Angjelichinoski, K. F. Trillingsgaard, and P. Popovski, "A statistical learning approach to ultra-reliable low latency communication," IEEE Transactions on Communications, vol. 67, no. 7, pp. 5153–5166, 2019.

RAMONI ADEOGUN received the B.Eng in Electrical and Computer Engineering from Federal University of Technology, Minna, Nigeria and a PhD in Electronic and Computer Systems Engineering from Victoria University of Wellington, New Zealand. He is currently an Assistant Professor with the Wireless Communication Networks (WCN) Section, Aalborg University, Denmark. Since 2020, he has also been an External Research Engineer with Nokia Bell Labs, Aalborg. Prior to joining Aalborg University, he has also worked in various positions at University of Cape Town, South Africa, Odua Telecoms Ltd, Nigeria, Izon Science Limited, Christchurch, New Zealand and National Space Research and Development Agency, Nigeria. His research interests include channel characterization, machine learning and AI for communications, radio resource allocation, intelligent spectrum access and interference management. He is a senior member of the IEEE and has co-authored over 40 international publications, including conference proceedings, and journal contributions.

GILBERTO BERARDINELLI received the first and second level degrees (cum laude) in telecommunication engineering from the University of L'Aquila, Italy, in 2003 and 2005, respectively, and the Ph.D. degree from Aalborg University, Denmark, in 2010. He is currently an Associate Professor with the Wireless Communication Networks (WCN) Section, Aalborg University, and also working in tight cooperation with Nokia Bell Labs. His research interests are mostly focused on physical layer, medium access control, and radio resource management design for 5G systems and beyond. He is the author or coauthor of more than 100 international publications, including conference proceedings, journal contributions, and book chapters.

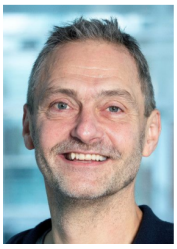

PREBEN E. MOGENSEN is Principal Scientist in the Standardization Research Lab of Nokia Bell Labs. He received the M.Sc. and Ph.D. degrees from Aalborg University, in 1988 and 1996, respectively. Since 1995, he has been part-time associated with Nokia in various research positions and have made contributions from 2G to 5G cellular technologies. He has been at Aalborg University since graduation in 1988. In 2000 he became Full Professor with Aalborg University, where he is currently leading the Wireless Communication Networks Section, Department of Electronic Systems. He has co-authored over 400 papers in various domains of wireless communication, and his Google Scholar h-index is 63. His current research interest includes industrial use cases for 5G, 5G evolution and 6G. He is a Bell Labs Fellow.